Acta Pharmacol Sin 2007 Nov; 28 (11): 1827–1834

Blackwell Publishing

Full-length article

A novel homospermidine conjugate inhibits growth and induces apoptosis in human hepatoma cells[1]

Song-qiang XIE[2,3], Ying-liang WU[2], Peng-fei CHENG[4], Min-wei WANG[2], Guang-chao LIU[5], Yuan-fang MA[5], Jin ZHAO[4], Chao-jie WANG[4,6]

[2]Department of Pharmacology, Shenyang Pharmaceutical University, Shenyang 110016, China; [3]Pharmacy College, Henan University, Kaifeng 475001, China; [4]Institute of Natural Products and Medicinal Chemistry, Henan University, Kaifeng 475001, China; [5]Medical College, Henan University, Kaifeng 475001, China

Key words

polyamine; apoptosis; cell cycle; mitochondrial membrane potential; caspase; Bcl-2

[1] Project supported by grants from the National Natural Science Foundation of China (No 20472016) and Henan Natural Science Foundation (No 512001300).
[6] Correspondence to Prof Chao-jie WANG.
Phn 86-378-388-0680.
E-mail wcjsxq@yahoo.com

Received 2007-01-24
Accepted 2007-04-04

doi: 10.1111/j.1745-7254.2007.00639.x

Abstract

Aim: To elucidate the mechanism responsible for the antiproliferative effects of a novel homospermidine conjugate, anthracenylmethyl homospermidine (ANTMHspd), in the human hepatoma BEL-7402 cell line. **Methods:** The viability of the cells was assessed by MTT assay and the trypan blue dye exclusion method. Morphological changes were observed by fluorescence microscopy with Hoechst 33258 staining. Cell cycle distribution, apoptosis, and mitochondrial membrane potential were measured by flow cytometry. Protein expression was detected by Western blot analysis. **Results:** ANTMHspd strongly decreased BEL-7402 cell proliferation in a dose- and time-dependent manner. Hoechst 33258 staining and the flow cytometry assay showed that ANTMHspd induced cell apoptosis and cell cycle perturbation. Furthermore, ANTMHspd could induce mitochondrial membrane potential loss and cytochrome c release and enhance cleaved caspase-3, cleaved caspase-9, and Bax protein expression without caspase-8 activation. ANTMHspd could also decrease the expression of Bcl-2 and cytochrome c in mitochondria. In addition, the specific inhibitors of caspase-9 and caspase-3 almost abolished the ANTMHspd-induced caspase-9 and caspase-3 activation, respectively. **Conclusion:** ANTMHspd could induce BEL-7402 cell apoptosis via the mitochondrial/caspase-dependent pathway and the Bcl-2 family was involved in the control of apoptosis.

Introduction

The naturally occurring polyamines, namely putrescine, spermidine, and spermine, play a crucial role in cell growth[1], such as the activation of kinases involved in the signal transduction pathway, the regulation of ion channel gating, and the modulation of oxidative processes[2]. Cells have complex regulatory mechanisms that control intracellular polyamine levels via transport, degradation, and biosynthesis[3]. Rapidly-dividing cells need large amounts of polyamines in order to grow, which can be realized by internal biosynthesis and/or external uptake via the active polyamine transporter (PAT). The elevated requirement of tumor cells for polyamines makes the polyamine pathway attractive for tumor-targeted chemotherapy[4].

Polyamines are also potential carriers for drug delivery because the polyamine transporter in tumor cells seems to have a wide structural tolerance of the substrates. In this regard, the antineoplastic drugs are conjugated to polyamines to facilitate their entrance into cells with active PAT. Several related polyamine-drug conjugates were designed to increase the cytotoxicity to tumor cells and reduce the side-effects on normal cells[5]. Previous efforts revealed that the non-native triamine, homospermidine, showed a better PAT recognition than natural polyamines. A leading conjugate, anthracenylmethyl homospermidine (ANTMHspd), was found to display an excellent PAT selectivity and strong inhibitory effects on several tumor cell lines[6]. Many reports revealed

that alkyl polyamine analogues exhibited cytotoxicity via apoptosis[7,8], however, the antiproliferative mechanism of the homospermidine conjugates has not been elucidated until now. In this study, the antitumor potency of ANTMHspd was investigated in the human hepatoma BEL-7402 cell line. The data demonstrated that ANTMHspd inhibited growth effectively and induced apoptosis in BEL-7402 cells.

Materials and methods

Materials All chemicals were purchased from Sigma (St Louis, MO, USA), unless otherwise indicated. RPMI-1640 and fetal calf serum (FCS) were purchased from Gibco (Grand island, NY, USA). The primary antibodies against caspase-3, caspase-8, caspase-9, cytochrome c, Bcl-2, Bax, as well as peroxidase-conjugated goat antimouse or antirabbit secondary antibody, were purchased from Santa Cruz Biotechnology (Delaware Avenue Santa Cruz, CA, USA). Z-DEVD-fmk (caspase-3 inhibitor) and Z-LEHD-fmk (caspase-9 inhibitor) were purchased from Imgenex (Suite E San diego, CA, USA). ANTMHspd (Figure 1) was provided by Prof WANG (Institute of Natural Products and Medicinal Chemistry, Kaifeng, China). The stock solution (10 mmol/L) was prepared in DMSO and diluted to various concentrations with serum-free culture medium.

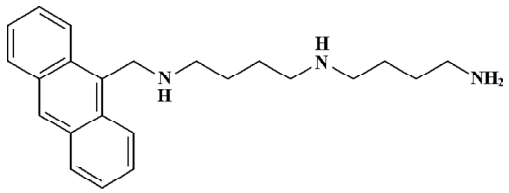

Figure 1. Structure of ANTMHspd.

Cell culture The human hepatoma BEL-7402 cell line, obtained from American Type Culture Collection (ATCC, Rockville, MD, USA), was cultured in RPMI-1640 supplemented with 10% heat-inactivated FCS and antibiotics (100 units/mL penicillin and 100 μg/mL streptomycin sulfate) at 37 °C in an atmosphere of 95% air and 5% CO_2 under humidified conditions. 1 mmol/L aminoguanidine was added as an inhibitor of amine oxidase derived from FCS and had no effect on the various parameters of the cells measured in this study[9].

Evaluation of cell viability and proliferation

MTT assay Chemosensitivity was assessed using the thiazolyl blue tetrazolium bromide (MTT) assay[1]. Briefly, 5000 exponentially growing cells were seeded onto 96-well, flat-bottomed plates and allowed to attach overnight. The cells were treated with the indicated concentrations of ANTMHspd for 48 h and 100 μL MTT (1 mg/mL) was added to each well. After incubation at 37 °C for 4 h, the MTT solution was removed and the crystals of the viable cells were dissolved with DMSO. The absorbance of each well was read at 570 nm.

Growth inhibition assay The exponentially growing cells were seeded onto 24-well, flat-bottomed plates at a density of 5×10^4/mL and allowed to attach overnight. The cells were treated with the indicated concentrations of ANTMHspd for different times. The cells were collected by trypsinization at different time points (d 1, 2, 3, 4, and 5) and counted by a Thoma hemocytometer (Shanghai, China) using the trypan blue dye exclusion method for viability.

Apoptosis and cell cycle analysis Apoptosis was quantified by assessing the fraction of cells with a sub-G_1 DNA content by flow cytometry. The cells were seeded in 25cm^2 flasks and then pre-incubated in RPM-I1640 supplemented with 0.2% FCS for 24 h which induced cell cycle synchronization[10]. The synchronous cells were treated with the indicated concentrations of ANTMHspd. After incubation for 24 or 36 h, the cells were washed twice with ice-cold phosphate-buffered solution (PBS), fixed, and permeabilized with ice-cold 70% ethanol at -20 °C overnight. The cells were treated with 50 μg/mL RNase A at room temperature for 30 min after being washed with ice-cold PBS, and finally stained with 50 μg/mL propidium iodide (PI) in the dark at 4 °C for 30 min. The distribution of the cell cycle phases with different DNA contents was read in a flow cytometer. Ten thousand events were acquired in each sample[11].

Hoechst staining of nuclear chromatin The cells were fixed with 4% formaldehyde in PBS at 37 °C for 10 min and permeabilized with a 19:1 mixture of ethanol/acetic acid at -20 °C for 15 min. The fixed cells were stained with 1 μg/mL Hoechst 33258 in PBS at room temperature for 20 min. The Hoechst-stained cells were analyzed by fluorescence microscopy[1].

Assessment of the change in mitochondrial membrane potential The mitochondria membrane potential (MMP) was measured using flow cytometry with rhodamine 123 (Rh123) and PI double staining. Rh123 accumulates in normal mitochondria due to its high negative charge and the reduction of MMP leads to the release of Rh123. Rh123 was dissolved in DMSO and diluted in PBS before treatment. About 1×10^6 cells were harvested by trypsinization, washed twice with PBS, and incubated with Rh123 (10 μg/mL) at 37 °C for 30 min in the dark. PI (10 μg/mL) was then added to the

cells and the cells were incubated for 5 min in the dark. The samples were analyzed by flow cytometry with a 15 mw argon laser at 488 nm. Fluorescence intensity was detected at the wavelength of 575 nm and 610 nm, respectively. The percentage of $Rh123^{-}/PI^{+}$ and $Rh123^{-}/PI^{-}$ presented the effective collapsed MMP[12].

Caspase activity assay The cell pellets were washed with ice-cold PBS and resuspended in 100 mmol/L Hepes buffer (pH 7.4), which contained protease inhibitors (5 μg/mL aprotinin and pepstatin, 10 μg/mL leupeptin, and 0.5 mmol/L phenylmethanesulfonyl fluoride). The cell suspension was lysed by 3 freeze-thawed cycles and the cytosolic fraction was obtained by centrifugation at 12 000×*g* at 4 °C for 20 min. DEVDase, IETDase, and LEHDase activities were evaluated by measuring proteolytic cleavage of chromogenic substrates Ac-DEVD-pNA, Ac-IETD-pNA, and Ac-LEHDpNA, which were used as the substrates for caspase-3, caspase-8, and caspase-9-like proteases, respectively. Briefly, the cell lysate (50 mg of protein) was added into the buffer containing 150 mol/L Ac-DEVD-pNA, Ac-IETD-pNA, and Ac-LEHD-pNA to a final volume of 150 μL. The reaction mixture was incubated at 37 °C for 1 h. The absorbance of enzymatically-released pNA was measured at 405 nm on a microplate reader every 20 min[13].

Western blotting The cells, treated with different concentrations of ANTMHspd for the desired exposure time, were harvested by trypsinization and washed with PBS. For the caspase inhibitor analysis, the cells were pretreated with 50 μmol/L Z-DEVD-fmk or Z-LEHD-fmk for 2 h, and then exposed with ANTMHspd for 24 h. Cytosolic and mitochondrial fractions were prepared as described[14]. Briefly, the cells were resuspended in 300 μL buffer (2 mmol/L Hepes-potassium hydroxide (KOH) [pH 7.5], 10 mmol/L $MgCl_2$, 1 mmol/L ethyleneglycol bis(2-aminoethyl ether)tetraacetic acid (EGTA), 1 mmol/L dithiothreito (DTT), and 250 mmol/L sucrose and protease inhibitor). After homogenization, the unbroken cells, large plasma membrane pieces, and nuclei were removed by centrifugation at 1000×*g* for 10 min. The supernatant was subjected to centrifugation at 10 000×*g* for 20 min. The pellet fraction containing mitochondria was resuspended in 500 μL buffer (10 mmol/L Tris-acetate [pH 8.0], 0.5% Nonidet NP-40, and 5 mmol/L $CaCl_2$). The supernatant was further centrifuged at 50 000×*g* for 2 h to generate cytosol. The detection of cytochrome c in the cytosolic and mitochondria fractions was analyzed by Western blotting. Total cellular protein was isolated using the protein extraction buffer (containing 150 mmol/L NaCl, 10 mmol/L Tris [pH 7.2], 5 mmol/L EDTA, 0.1% Triton-100, 5% glycerol, and 2% SDS). The protein concentrations were determined using the protein assay kit. Equal amounts of proteins (50 μg/lane) were fractionated using 12% SDS-PAGE and transferred to polyvinylidene difluoride (PVDF) membranes. The membranes were incubated with primary antibodies against caspase-3, caspase-8, caspase-9, cytochrome c, Bcl-2, and Bax (1:5000). After being washed with PBS, the membranes were incubated with peroxidase-conjugated goat antimouse or antirabbit secondary antibody (1:3000), followed by enhanced chemiluminescence staining through the enhanced chemiluminescence system. Actin was used to normalize protein loading[1].

Statistical analysis Results from at least 3 independent experiments were given as mean±SD. Statistical significance was done using the ANOVA test. Results were considered significant when $P<0.05$.

Results

Inhibition of growth by ANTMHspd In the present study, ANTMHspd exhibited a dose- and time-dependent growth inhibition against BEL-7402 cells at the dose of 0.1–50 μmol/L (Figure 2). The 50% inhibiting concentration (IC_{50}) value for the BEL-7402 cells was 0.56±0.08 μmol/L for a 48 h treatment. The proliferation of the BEL-7402 cells was gradually attenuated with the prolonged treatment time of ANTMHspd (Figure 3).

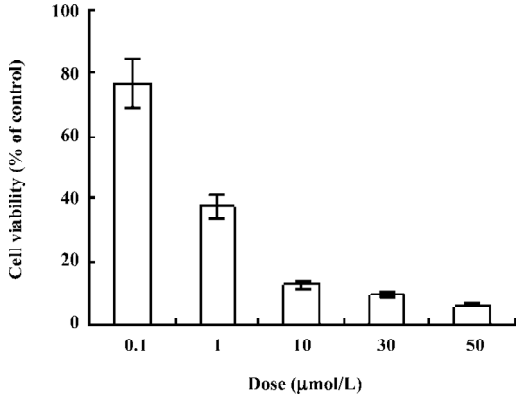

Figure 2. Inhibition of proliferation of ANTMHspd to BEL-7402 cells assessed by MTT. After 24 h adherence, the cells were treated with different concentrations of ANTMHspd for 48 h. Each value represents mean±SD in 3 independent experiments.

Cell cycle perturbation by ANTMHspd A flow cytometry DNA analysis revealed that ANTMHspd induced cell cycle perturbation (Figure 4). The detailed data concerning the percentage of sub-G_1 cells and cell cycle distribution of BEL-

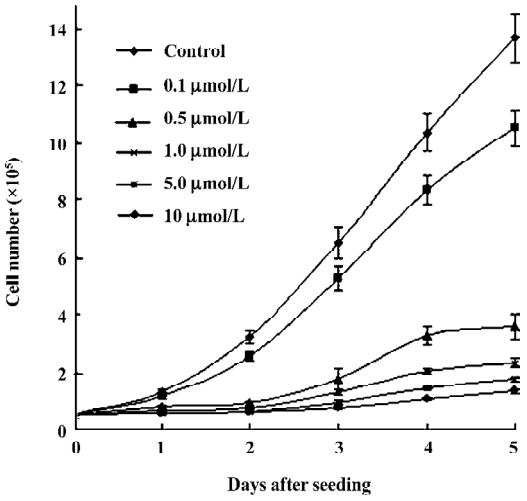

Figure 3. Growth inhibition of ANTMHspd on cells assessed by trypan blue dye exclusion. After 24 h adherence, the cells were treated with different concentrations of ANTMHspd at different times. Each value represents mean±SD in 3 independent experiments.

7402 cells treated with ANTMHspd are shown in Table 1. Compared to the control (untreated cells), changes in the cell cycle distribution of treated BEL-7402 cells were evident. This was accompanied by an increase in the sub-G_1 region of cells with a fractional DNA content.

Effect of ANTMHspd on cell morphology To determine whether or not the sub-G_1 fraction, affected by ANTMHspd, was related to apoptosis, both the control and ANTMHspd-treated cells were stained with the fluorescent dye Hoechst 33258 and visualized by fluorescence microscopy. Typical morphological changes of apoptosis, including chromatin condensation, dense chartreuse nucleolus, and nuclear fragmentation, were observed in the treated cells, but not in the control cells (Figure 5).

Assessment of the change in MMP In Figure 6, the lower left quadrant represented the percentage of $Rh123^-/PI^-$ cells, the higher left quadrant represented the percentage of $Rh123^-/PI^+$ cells, the lower right quadrant represented the percentage of $Rh123^+/PI^-$ cells, and the higher right quadrant represented the percentage of $Rh123^+/PI^+$ cells which reflected the damaged cells. Most untreated cells have intact plasma membrane and normal MMP. After being treated with the indicated concentrations of ANTMHspd for 12 or 24 h, $Rh123^-/PI^-$ and $Rh123^-/PI^+$ cells exhibited a dose- and time-dependent increase (Figure 6). These results indicated that BEL-7402 cells lost MMP and membrane integrity. For example, the percentage of MMP collapse reached 70.25% after the cells were treated with 5 μmol/L ANTMHspd for 24 h (Table 2).

Effect of ANTMHspd on apoptosis-related proteins The activity of caspase-9 and caspase-3 was significantly increased compared with untreated cells in a dose- and time-dependent manner, while ANTMHspd had no effect on the activity of caspase-8 (Figure 7). These results were confirmed by Western blotting. ANTMHspd treatment increased the cleavage of caspase-9 and caspase-3 in a dose- and time-

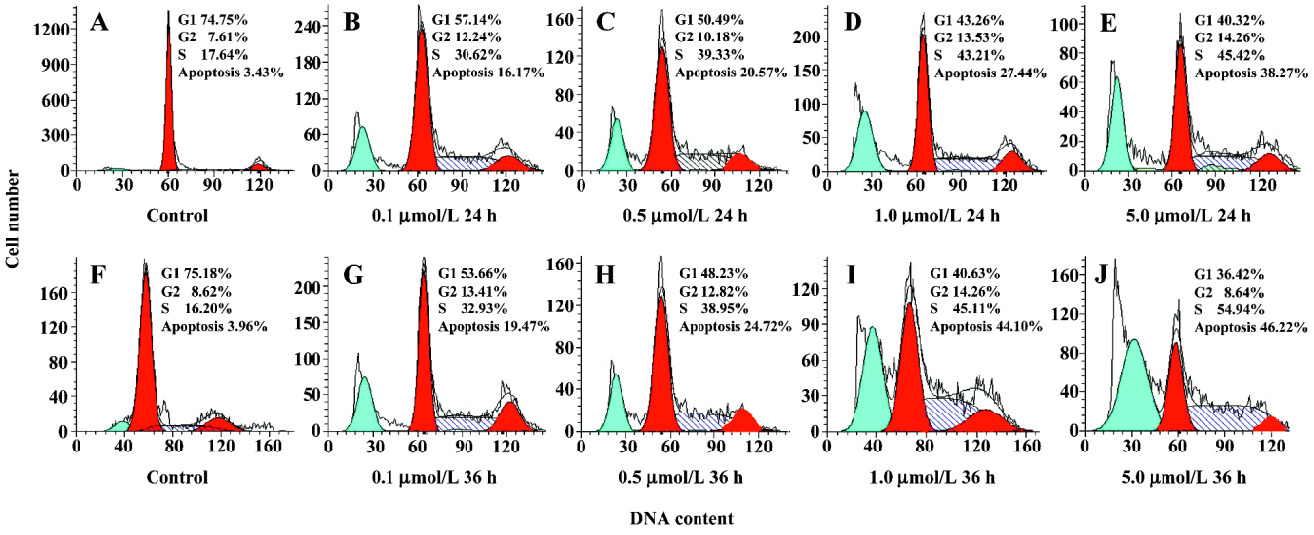

Figure 4. Inhibition of cell cycle progress in BEL-7402 cells treated with ANTMHspd for 24 or 36 h. Cells were fixed with ethanol and stained with PI. Cell cycle distribution was analyzed by flow cytometry. First peak represents sub-G_1 peak, which was taken as the fraction of the apoptotic cell population.

Table 1. Effect on cell-cycle phase distribution of BEL-7402 cells treated with different concentrations of ANTMHspd at different times. Each value represents mean±SD in 3 independent experiments. $^{b}P<0.05$, $^{c}P<0.01$ *vs* control.

Dose (μmol/L)	Time (h)	G_0/G_1 (%)	G_2/M (%)	S (%)	Apoptosis rate
0	–	75.14±2.06	7.53±0.84	17.33±1.13	3.46±0.47
0.1	24	56.73±2.14^{b}	12.76±1.15^{c}	30.51±1.76^{b}	16.92±1.43^{b}
0.5	24	49.26±1.94^{b}	10.08±0.92^{c}	40.66±1.61^{b}	21.17±0.94^{b}
1.0	24	42.63±2.43^{b}	13.92±0.23^{c}	43.45±2.05^{b}	27.15±1.36^{b}
5.0	24	39.28±1.62^{b}	15.06±1.04^{c}	45.66±1.94^{b}	39.25±1.47^{b}
0.1	36	53.85±2.19^{b}	12.84±1.21^{c}	33.31±1.25^{b}	20.29±1.16^{b}
0.5	36	48.24±1.82^{b}	12.17±0.96^{c}	38.59±1.43^{b}	25.28±1.25^{b}
1.0	36	40.87±1.36^{b}	13.88±1.09^{c}	45.25±2.31^{b}	43.87±2.93^{b}
5.0	36	36.98±1.27^{b}	8.47±0.81	54.55±2.83^{b}	47.38±1.84^{b}

Table 2. Changes in the mitochondrial membrane potential of BEL-7402 cells treated with different concentrations of ANTMHspd at different times. Each value represents mean±SD in 3 independent experiments. $^{b}P<0.05$, $^{c}P<0.01$ *vs* control.

Dose (μmol/L)	Time (h)	$Rh123^{-}/PI^{+}$	$Rh123^{-}/PI^{-}$	Total
0	–	0.65±0.06	0.91±0.07	1.52±0.16
0.1	12	2.46±0.27^{c}	2.53±0.37^{c}	5.06±0.42^{c}
0.5	12	7.65±1.04^{c}	9.51±0.39^{b}	17.68±1.27^{b}
1.0	12	9.21±1.29	13.06±0.41^{b}	23.24±1.75^{b}
5.0	12	23.28±1.54^{b}	31.75±1.76^{b}	54.69±1.48^{b}
0.1	24	13.18±1.39^{b}	9.81±0.69^{b}	23.62±1.52^{b}
0.5	24	15.63±1.61^{b}	13.47±0.53^{b}	28.94±1.67^{b}
1.0	24	18.73±1.55^{b}	34.88±1.97^{b}	52.67±2.26^{b}
5.0	24	17.42±0.95^{b}	51.76±2.49^{b}	68.94±3.91^{b}

dependent manner. The expression of cleaved-caspase-8 was undetectable in ANTMHspd-treated cell and was detected in the positive control cell (5×10^{8} U/L TNF-α-treated cell). The cytochrome c release from mitochondria was enhanced concomitant with the related attenuation of cytochrome c in mitochondria. The Bcl-2 protein expression was downregulated and Bax was upregulated from 24 to 48 h (Figure 8). In addition, the specific inhibitors of caspase-9 and caspase-3 almost completely abolished the ANTMHspd-induced cleavage of caspase-9 and caspase-3, respectively (Figure 9).

Discussion

A recent review pointed out new polyamine derivatives as potent therapeutic agents[15]. The roles of alkyl polyamine analogues in apoptosis have been investigated in a number of experimental systems. The results indicated that polyamine analogues could produce cytotoxicity through apoptosis[7,8], but the related functions of polyamine conjugates are rarely elucidated.

Some data demonstrated that polyamine analogues activated a classical apoptosis response, including the release of cytochrome c and the activation of the caspase cascade,

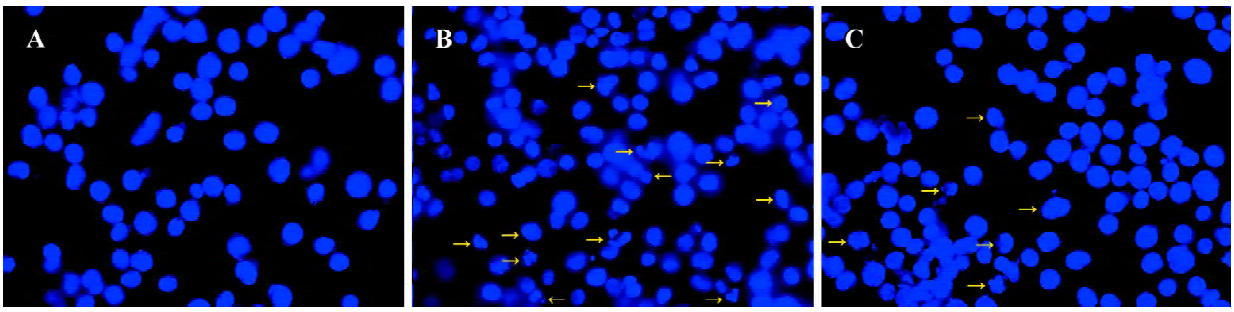

Figure 5. Morphological observation of BEL-7402 cells treated for 24 h by fluorescence microscopy (×400 magnification). Cells were stained with Hoechst 33258. (A) untreated cells; (B) 1.0 μmol/L treated cells; (C) 0.5 μmol/L treated cells.

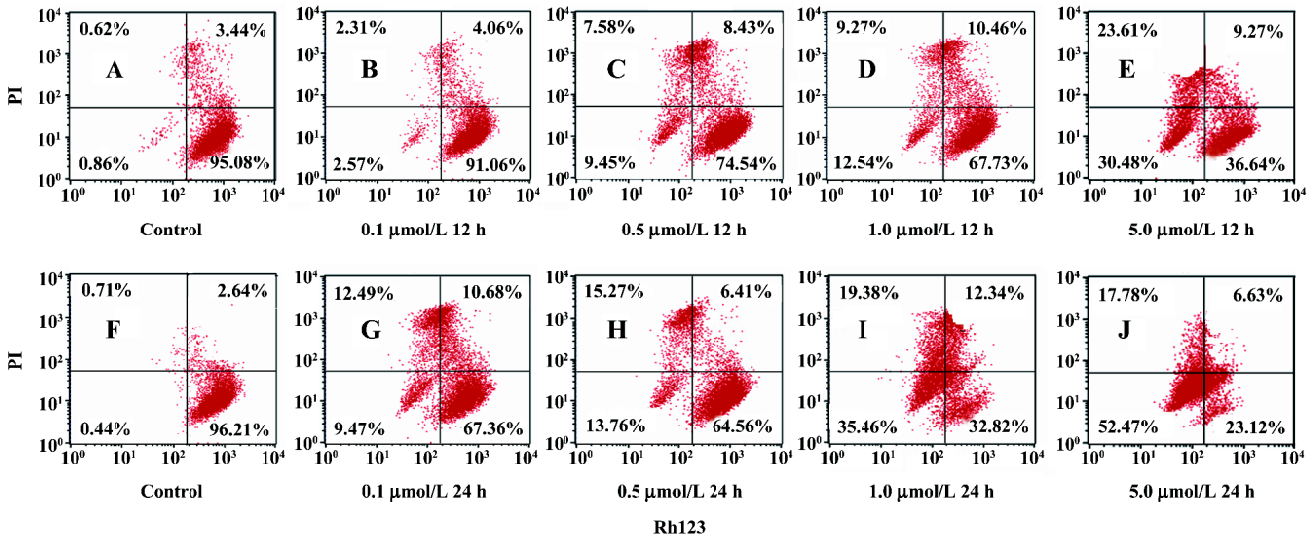

Figure 6. Changes in the mitochondrial membrane potential of BEL-7402 cells induced by ANTMHspd.

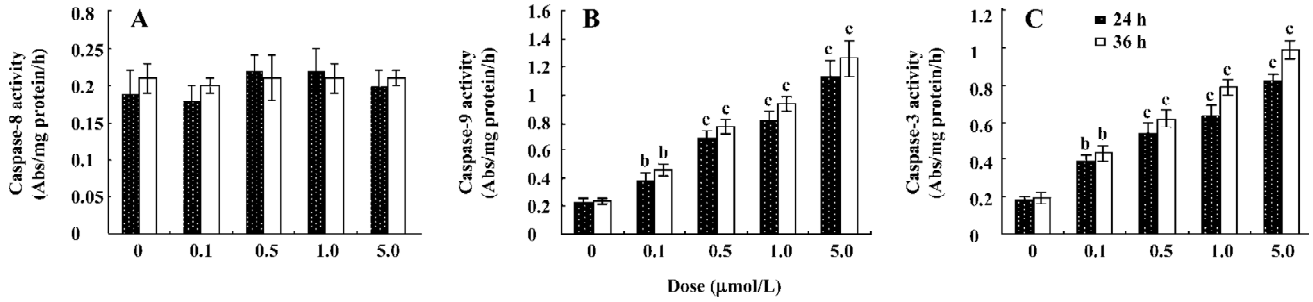

Figure 7. Effect of ANTMHspd on the activation of caspase-8 (A), caspase-9 (B), and caspase-3 (C). BEL-7402 cells were treated with ANTMHspd at different concentrations and at different times. Each value represents mean±SD in 3 independent experiments. $^{b}P<0.05$, $^{c}P<0.01$ *vs* control.

which initiated the morphological and biochemical steps in the apoptosis pathway[16]. In this study, we found that ANTMHspd could inhibit BEL-7402 cell proliferation with an IC_{50} value of 0.56±0.08 μmol/L at 48 h. This revealed that ANTMHspd might be a potential leading agent with a structure different from the alkyl polyamine analogues[1]. To explore the mechanism responsible for the antiproliferative effects of ANTMHspd, the changes of cell morphology were first assessed. After being treated with different concentrations of ANTMHspd, the morphology of BEL-7402 cells changed obviously, including cell shrinkage, nuclear fragmentation, as well as chromatin condensation. A flow cytometry DNA analysis revealed that ANTMHspd induced a sub-G_1 cell population and cell cycle perturbations. These results indicated that ANTMHspd could induce BEL-7402 cell apoptosis.

Apoptosis can be triggered by several stimuli and is controlled by 2 major pathways, namely the mitochondrial pathway and membrane death receptor pathway[17]. In the mitochondrial pathway, mitochondria have a crucial position in apoptosis control. The loss of MMP induces cytochrome c release from the mitochondria to the cytoplasm, which leads to the activation of caspase-9 and downstream cleavage of caspase-3. The membrane death receptor pathway is characterized by the binding between cell death ligands and cell death receptors and the subsequent activation of caspase-8 and caspase-3.

To reveal the precise molecular mechanism of ANTMHspd-induced apoptosis in BEL-7402 cells, we observed the effect of ANTMHspd on MMP, cytochrome c, the activity of caspases, as well as the Bcl-2 family. The present results showed that ANTMHspd decreased MMP and increased

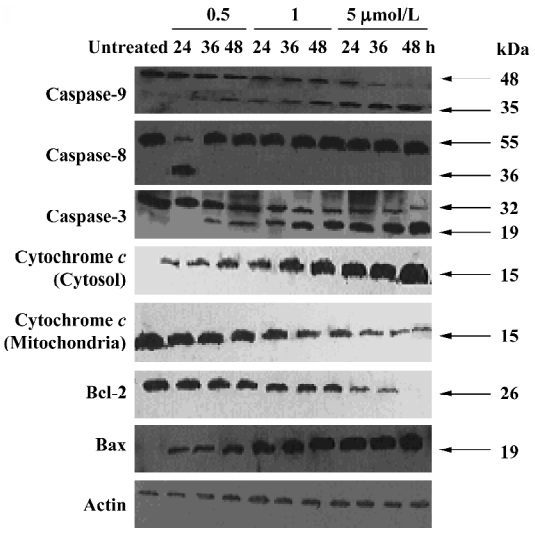

Figure 8. Expression of caspase-3, caspase-8, caspase-9, cytochrome c, Bcl-2, and Bax in BEL-7402 cells treated with ANTMHspd at the indicated doses and times. In caspase-8, lane 2 represents TNF-α treatment as the positive control. Equal amounts (50 μg/lane) of cellular protein were fractionated on 12% SDS-PAGE gels and transferred to PVDF membranes. Actin protein was blotted as a control.

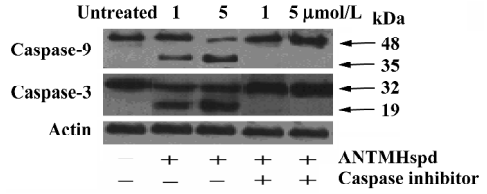

Figure 9. Effect of caspase-9 inhibitor (Z-LEHD-fmk) and caspase-3 inhibitor (Z-DEVD-fmk) on ANTMHspd-induced apoptosis. Equal amounts (50 μg/lane) of cellular protein were fractionated on 12% SDS-PAGE gels and transferred to PVDF membranes. Actin protein was blotted as a control.

the level of cytochrome c in the cytoplasm with the corresponding decrease of cytochrome c in mito-chondria. To determine whether caspases are involved in the ANTMHspd-induced apoptosis in BEL-7402 cells, the catalytic activity of caspase-8, caspase-9, caspase-3, as well as their expression were measured. The data demonstrated that ANTMHspd could activate caspase-9 and caspase-3. However, the activity of caspase-8, an apoptosis-initiating protease linked to the death receptors, was unchanged and the cleaved fragment of caspase-8 was not detected. It was suggested that ANTMHspd induced apoptosis via the mitochondrial pathway, but not the membrane death receptor pathway. Furthermore, to determine whether the activation of caspases is essential for ANTMHspd-mediated apoptosis, pre-incubation with specific inhibitors of caspase-9 and caspase-3 almost abolished the ANTMHspd-induced caspase-9 and caspase-3 activation respectively. This confirmed that ANTMHspd induced apoptosis in a caspase-dependent manner. However, BE-3-3-3, a *bis*(ethyl)norsper-mine, induces breast cancer cell apoptosis via both the membrane death receptor pathway and mitochondrial pathway because BE-3-3-3 can activate caspase-9, caspase-3, and caspase-8 in human breast cancer cells[18]. This different pathway demonstrates that the ability of polyamine analogues to induce apoptosis is dependent on the characteristics of the cell line.

The Bcl-2 family plays a central role in regulating the mitochondrial apoptosis pathway. More than 20 Bcl-2 family members consist of anti-apoptosis membranes (including Bcl-2 and Bcl-xL) and pro-apoptosis membranes (including Bax and Bak) have been identified. Bcl-2 is an important element during apoptosis mediated by the mitochondrial pathway and has been identified as preventing cytochrome c release from the mitochondria. In contrast, Bax can induce the release of cytochrome c from the mitochondria[19]. The present report reveals that ANTMHspd-induced apoptosis is companied by an increased expression of Bax and a reduced protein level of Bcl-2 in BEL-7402 cells. Huang et al reported that other pathways but caspases can function as apoptosis effectors in brease cancer (MDA-MB-231 and MCF7) cells and that the regulation of Bcl-2 family members by polyamine analogue was cell type specific[1]. The effects of ANTMHspd on caspase activity and the expression of the Bcl-2 family in other cell lines will be carried out in our laboratory.

Taken together, we can conclude that ANTMHspd induced the apoptosis of BEL-7402 cells via the mitochondria/caspase-9/caspase-3 dependent pathway and the Bcl-2 family was involved in the control of apoptosis.

References

1 Huang Y, Hager ER, Dawn L, Dunn VR, Hacker A, Frydman B, *et al*. A novel polyamine analog inhibits growth and induces apoptosis in human breast cancer cells. Clin Cancer Res 2003; 9: 2769–77.

2 Nitta T, Igarashi K, Yamamoto N. Polyamine depletion induces apoptosis through mitochondria-mediated pathway. Exp Cell Res 2002; 276: 120–8.

3 Shah N, Antony T, Haddad S, Amenta P, Shirahata A, Thomas TJ, *et al*. Antitumor effects of bis(ethyl)polyamine analogs on mammary tumor development in FVB/NTgN (MMTV neu) transgenic mice. Cancer Lett 1999; 146: 15–23.

4 Casero RA, Woster PM. Terminally alkylated polyamine analogues as chemotherapeutic agents. J Med Chem 2001; 44: 1–26.

5 Garcia G, Sol V, Lamarche F. Synthesis and photocytotoxic

activity of new chlorin-polyamine conjugates. Bioorg Med Chem Lett 2006; 16: 3188–92.
6 Wang CJ, Delcros JG, Biggerstaff J, Phanstiel IV. Synthesis and biological evaluation of N1-(anthracen-9-ylmethyl)triamines as molecular recognition elements for the polyamine transporter. J Med Chem 2003; 46: 2663–71.
7 Davidson NE, Hahm HA, McCloskey DE, Woster PM, Casero RA Jr. Clinical aspects of cell death in breast cancer: the polyamine pathway as a new target for treatment. Cancer Res 1999; 6: 69–73.
8 McCloskey DE, Casero RA Jr, Woster PM, Davidson NE. Induction of programmed cell death in human breast cancer cells by an unsymmetrically alkylated polyamine analogue. Cancer Res 1995; 55: 3233–6.
9 Monti MG, Ghiaroni S, Barbieri D. 2-Deoxy-D-ribose-induced apoptosis in HL-60 cells is associated with the cell cycle progression by sperimidine. Biochem and Biophy Res Commun 1999; 257:460–5.
10 Kues WA, Anger M, Carnwath JW, Paul D, Motlik J, Niemann H. Cell cycle synchronization of porcine fetal fibroblasts: effects of serum deprivation and reversible cell cycle inhibitors. Biol Reprod 2000; 62: 412–9.
11 Chang HS, Yamato O, Yamasaki M. Growth inhibitory effect of alk(en)yl thiosulfates derived from onion and garlic in human immortalized and tumor cell lines. Cancer Lett 2005; 223: 47–55.
12 Ren DD, Peng GH, Huang HG. Effect of rhodoxanthin from *Potamogeton crispus L* on cell apoptosis in Hela cells. Toxicol *In Vitro* 2006; 20: 1411–8.
13 Min JK, Kim JH, Cho YL, Maeng YS, Lee SJ, Pyun BJ. 20(S)-Ginsenoside Rg3 prevents endothelial cell apoptosis via inhibition of a mitochondrial caspase pathway. Biochem Biophy Res Commun 2006; 349: 987–94.
14 Eguchi Y, Srinnivasn A, Tomaselli KJ, Shimizu S, Tsujimoto Y. ATP-dependent steps in apoptotic signal transduction. Cancer Res 1999; 59: 2174–81.
15 Lin KT, Dance AM, Bestwick C. The biological activities of new derivatives as potent therapeutic agents. Biochem Soc Trans 2003; 31: 407–10.
16 Ha HC, Woster PM, Casero RA. Release of cytochrome *c* from mitochondria in polyamine analogue induced program cell death. Cancer Res 1979; 39: 451–6.
17 Hegardt C, Andersson G, Stina M. Oredsson. Different roles of spermine in glucocorticoid and Fas-induced apoptosis. Exp Cell Res 2001; 266: 333–41.
18 Hegardt C, Johannsson OT, Oredsson SM. Rapid caspase-dependent cell death in cultured breast cancer cells induced by the polyamine analogue N^1,N^{11}-diethylnorspermine. Eur J Biochem 2002; 269: 1033–9.
19 Liu J, Li Y, Ren W. Apoptosis of HL-60 cells induced by extracts from Narcissus tazetta Var chinensis. Cancer Lett 2006; 242: 133–40.